



This open access document is published as a preprint in the Beilstein Archives with doi: 10.3762/bxiv.2019.100.v1 and is considered to be an early communication for feedback before peer review. Before citing this document, please check if a final, peer-reviewed version has been published in the Beilstein Journal of Organic Chemistry.

This document is not formatted, has not undergone copyediting or typesetting, and may contain errors, unsubstantiated scientific claims or preliminary data.

Preprint Title The reaction of anthracyl- α -hydroxyphosphonate with anthracene: Facile Access to diverse (*bis*)-anthracylphosphonates as a suitable source for useful extensive π -conjugates

Authors Moghal Z. K. Baig, Banchanidhi Prusti, Shouvik Bhui and Manab Chakravarty

Publication Date 06 Sep 2019

Article Type Full Research Paper

Supporting Information File 1 Supporting Information_MC.docx; 3.7 MB

ORCID® iDs Banchanidhi Prusti - <https://orcid.org/0000-0003-4489-2509>; Manab Chakravarty - <https://orcid.org/0000-0001-8604-7886>

The reaction of anthracyl- α -hydroxyphosphonate with anthracene: Facile Access to diverse (*bis*)-anthracylphosphonates as a suitable source for useful extensive π -conjugates

Moghal Zubair Khalid Baig, Banchanidhi Prusti, Shouvik Bhui and Manab Chakravarty*

Address: ¹Department of Chemistry, Birla Institute of Technology and Science-Pilani, Hyderabad Campus, Jawaharnagar, Shamirpet, Hyderabad, India, 500078

Email: manab@hyderabad.bits-pilani.ac.in

* Corresponding author

Abstract

Molecular anthracene has been used as arene in the Friedel-Crafts (FC) type arylation reaction of anthracyl- α -hydroxyphosphonate in the presence of acid. A diverse product formation is observed, in which anthracene unit is found to be linked through its C1 position with α -C of phosphonate. Interestingly, the molecular conformation (X-ray structure) of this phosphonate reveals one of the bond angles of a tetrahedral carbon as 118° which is close to the C of sp^2 character. The attacks from C1, C2 or C9 nucleophilic center of molecular anthracene to C10 atom of 9-anthrylphosphonate are also recognized. The diverse molecular structures are established spectroscopically. The bis-anthracyl compounds with a P-CH₂ unit have been successfully utilized in Horner-Wadsworth-Emmons (HWE) reactions to afford extensive bis-anthracyl-linked π -conjugates. Thus, the electronically different

substituent is attached to the system by varying the aldehydes. Among all these π -conjugates, the compound with three anthracyl core is noticed as a weak AIEgen (Aggregation-Induced emission active fluorogen).

Keywords

Anthracene, C-C bond formation, Phosphonate, π -conjugates, Aggregation-Induced emission

Introduction

The link of phosphonates with anthracene (Anth) core (see Fig 1) offered a significant number of molecules with potential applications in the field of materials and biological sciences as presented in Figure 1.¹⁻² In particular, multi-anthracene assemblies brought attention to a large community as organic functional materials in terms of their unique photo-physical and, chemical behavior.³ In fact, the organic reactions associated with anthracene unit was found to be eye-catching.⁴ All these aspects of such unit made us develop new anthracene linked phosphonates through a Friedel-Crafts (FC) type arylation reaction of easily accessible anthracyl- α -hydroxyphosphonate **1** with arenes.⁵

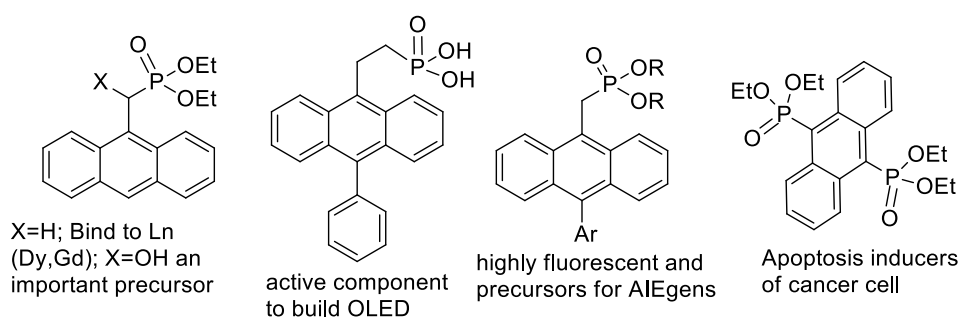


Fig 1. Reported anthracylphosphonates and their applications.

This method was proved to be much better than the earlier existing method in terms of the cost and operational simplicity.⁶ More importantly, such phosphonates were used in simple but effective Horner-Wadsworth-Emmons (HWE) reactions to generate anthracyl π -conjugates having potential applications in the field of materials science.⁷ In our recent engagement on the research of generating a variety of anthracene-based molecules as an effective AIEgens,^{7a,8} we report herein the FC-type arylation reaction of anthracyl- α -hydroxyphosphonate with anthracene as an arene in the presence of an acid with a drive to afford multi anthracyl-linked π -conjugates. Although the historically famous FC reactions are felt to be old-fashioned, the recent progress on FC reactions in the organic synthesis is still demanding.⁹ The anthracyl carbocation, the main species for the FC reactions, were well monitored before.^{4a-b} In this study, we have found the best economic path to bring multiple anthracyl units together as a part of the planar/non-planar conjugated system. Moreover, anthracyl π -conjugates are very well established as aggregation-induced emission (AIE) active fluorogens that are utilized in the field of optoelectronic applications.¹⁰ Some of these compounds are presented in Fig 2.

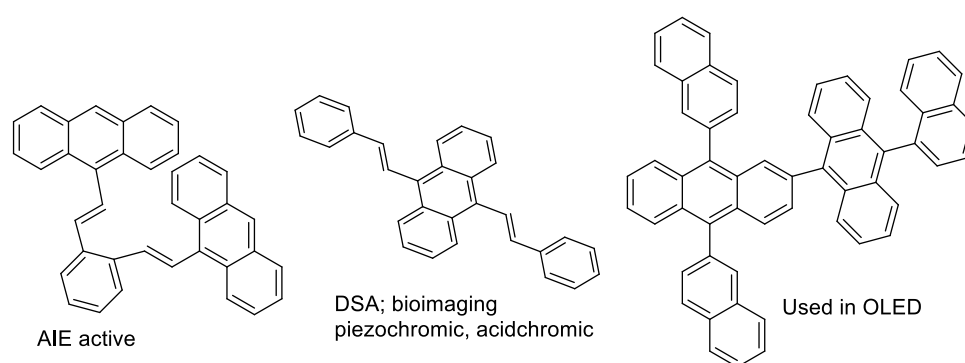


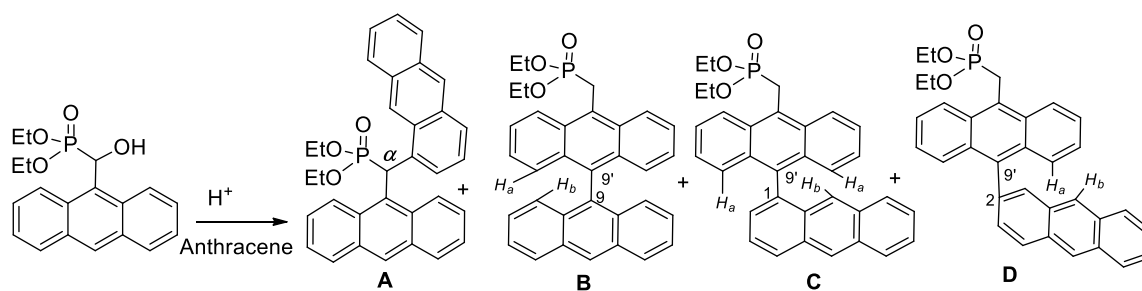
Fig 2 Reported anthracyl π -conjugates with applications

Many of these molecules are created *via* expensive metal-catalyzed coupling reactions. In fact, the link between anthracene and arene is established with multi-step, Pd-catalyzed tedious synthetic routes.^{7c-d} In this connection, we plan for facile

synthesis of new anthracene-linked anthracylphosphonates and utilize them in HWE reactions to generate anthracyl π -conjugates. Moreover, our observations on the variety of products reveal that this work is not the incremental rather it is found to be an easy way to bring multiple anthracyl cores within a molecule. The AIE-behavior have also been explored for these molecules.

Results and Discussion

From our earlier observations, the arylation at α -position was observed when α -hydroxyphosphonates were treated with activated/unactivated arenes.¹¹⁻¹² However, anthracene as an arene is quite interesting with its flat, rigid molecular structure and unusual reactivity.³⁻⁴ Anthracene unit has the possible scopes to attack different centers depending on the nucleophilicity of anthracenyl C's and the situation that controls the stability of the intermediate including the steric factors. In our initial attempt, FC-type arylation of anthracen-9-yl- α -hydroxyphosphonate with anthracene as an arene resulted possibly four products **A-D** as shown in scheme 1. Notably, the attack took place at α -carbon for **A** offering the -PCH(Anth)₂ unit and the other isomers **B-D** possess -PCH₂(Anth-Anth) unit. The formation of all these products is mainly governed by the stability of the carbocation intermediates, nucleophilicity and the steric factors (van der Waals interaction) amongst the anthracyl carbon centers, in particular, the repulsion between peripheral H's (H_a and H_b; **Scheme 1**). The compound **A** with a distinct R_f value [0.6 in 40% EtOAc/Hexane] is isolated in a pure form and characterized ambiguously (*vide infra*). However, we could not isolate the compounds **B-D** individually in pure form using column chromatography due to the overlapped R_f values ~0.3 in 40% EtOAc/Hexane. Therefore, we gave an effort to maximize the formation of one of these products by varying the reaction conditions.



Scheme 1: The attack of anthracene at different places; Synthesis of anthracylanthrylphosphonates

We have tried to optimize the yield of these compounds by varying reaction conditions as stated in this table (Table 1).

Table 1: Optimization table for the reaction of anthracene with phosphonate^a

Entry	Acid (equiv)	Time (hr)	Temp (°C)	Total conversion ^b (%) [isomeric products] ^c
1	<i>p</i> -TSA.H ₂ O (2)	24	25	NR ^d
2	CH ₃ SO ₃ H (2.2)	2	25	75% [A (40%), B , C , D mixture (60%)]
3	CH ₃ SO ₃ H (2.2)	2	0	70% [A (43%), B , C , D mixture (57%)]
4	FeCl ₃ . 6H ₂ O (2)	24	25	NR
5	FeCl ₃ (1)	3	25	20%
6	ZnCl ₂ (2)	24	25	NR
7	BF ₃ .OEt ₂ (2)	2	25	80% [A (15%); B (3%), C (75%): D (7%)] ^d
8	BF ₃ .OEt ₂ (2)	2	70	50% [A (8%); B (7%)+ C (79%): D (6%)] ^d
9	NiCl ₂ (2)	24	25	NR
10	CuCl ₂ .2H ₂ O (2)	24	25	NR
11	CF ₃ SO ₃ H (2)	2	25	80% [A (11%); B (9%); C (77%): D (3%)] ^d
12	BF ₃ .OEt ₂ (2)	24	0	NR
13	BF ₃ .OEt ₂ (2)	2	80	50% [A (5%); B (12%), C (79%), D (4%)] ^d

^aall the reactions were performed in dichloromethane except entry 8 where dichloroethane was used; ^bisomeric products ratio was calculated by integrating the respective signals, revealed in ¹H/³¹P NMR spectra; ^cNR: no reaction, starting material was recovered; ^dadditional small amount of impurities were observed possibly due to the formation of phosphonic acids.

The ³¹P-NMR spectrum for the reaction mixture for entry 11 (Fig S10) shows essentially four peaks at δ 25.8 (with a relatively larger area under the peak), 25.9, 25.7 and 25.6 along with peaks at δ 23.7 (unreacted starting material). Among these, signals at δ 25.8, 25.9 and 25.7 form a separate cluster while the peak at δ 25.6 is somewhat distinct (Fig S8) and found to be originated from the isolated compound **A**. Therefore, other three peaks must be due to the compounds **B-D** as depicted in scheme 1.

As anticipated, the arylation takes place at α -carbon to generate **A** (scheme 1) that was isolated in pure state (27% isolated yield) from the reaction mixture of entry 2 (Table 1). The compound **A** is characterized from the singlet at δ 8.24 for anthracyl-*H* at C10 and methine PCH proton (α) at δ 6.82 as a doublet with coupling constant (*J*) 30.4 Hz in ¹H NMR (Fig 3) as well as a doublet at δ 43.3 with *J* = 142.1 Hz for PCH in the ¹³C NMR spectra. Such a downfield signal for P-CH proton was earlier reported by us for pyrene substituted naphthylphosphonate compound.¹² The diamagnetic anisotropic effects of two anthracene rings bring this proton in the downfield region. Moreover, the molecular structure is confirmed by the single-crystal X-ray diffraction studies as shown in Fig 3. The molecular structure of **A** is an example of a compound that adjusts the molecular conformation in terms of the electronic and van der Waals interactions through a fantastic choice where C α (a *sp*³ carbon) prefers holding two anthracene rings through C1 and C9 atoms (Fig 3). Interestingly, two anthracene rings hang from C α by keeping the inter-planar angle

~86°. The bond angle for C1-C α -C9 is 118° that is closer to the bond angle for the sp^2 hybridized carbon. To the best of our knowledge, such example is not reported in the literature.

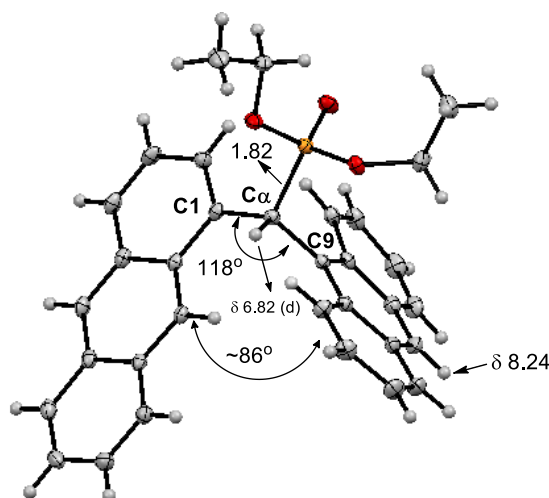


Fig 3 Molecular structure of compound **A** with selected bond distances (Å) and angles (°). The ¹H NMR signals for two specific protons are also mentioned.

The crystalline nature, R_f value in TLC and the distinct ³¹P/¹H NMR-signals of compound **A** are considerably different than that of P-CH₂ isomers **B-D**. Even the reaction mixture ³¹P-NMR spectrum also do not support the formation of other possible isomeric products of type **A** through C2 or C9 attack at C α .

Arylation at C10 position of anthracene results in the inseparable mixture of isomers (**B-D**) that is indicated through ³¹P-NMR spectrum of the reaction mixture. Upon screening with different acids (Table 1), the formation of compound **A** is found to be relatively preferred in the treatment with MeSO₃H at 0 °C or 25 °C, from which we could isolate **A** in pure form with 27% yield. We have further explored a few other acids where F₃B.OEt₂ (entries 7-8) maximizes the yield of a mixture of **B-D** (with PCH₂ unit) where one of them is found to be formed in major portion at room temperature. Through careful inspection of ¹H-NMR, we confirm the structure of a major product as **C**. The **B**, **C** and **D** regioisomers can easily be differentiated by analyzing the ¹H-NMR spectra. The formation of **C** as a major product is also further

supportive through mechanistic visions. A similar result is achieved under triflic acid treatment (entries 11). However, compound **C** is isolated with another isomer (**B**, as indicated in $^1\text{H-NMR}$) with the regioisomeric ratio **C/B**~75/25 as analyzed from the ^1H -(Fig S14-15) and $^{31}\text{P-NMR}$ spectra (Fig S17). The $^1\text{H-NMR}$ peak at δ 8.24 for C10-attached proton (assigned to anthracyl proton for compound **A**, Fig 3) is completely disappeared for these isomers, confirming the substitution occurs at C10. We could interpret the isomeric mixture of **C** and **B** from two different distinct doublets at δ 4.25 and 4.31 respectively with $J \sim 22$ Hz for PCH_2 protons in $^1\text{H-NMR}$ spectrum of the isolated compound (Fig 4). The unique P-C coupling was also observed in $^{13}\text{C-NMR}$ spectrum for two different signals at δ 27.3 and 27.4 as a doublet with $J \sim 140.7$ Hz for PCH_2 . Thus, the products with PCH and PCH_2 unit can easily be differentiated through $^{13}\text{C-NMR}$ where PCH (for **A**) appears at δ 43.3 and PCH_2 (for **B** and **C**) resonates at δ 27.3 (Fig 4). This observation is very much consistent with our previous reports.^{5,11} Unfortunately, no single crystals could be grown from this mixture of compounds **B** and **C** even after several attempts. Thus, the reaction conditions stated at entries 2 and 3 are used to afford **A** while entries 7 or 11 are applied to afford **C** as a regioisomeric mixture.

Assignment of the structure based on $^1\text{H NMR}$ -spectra

The structures of the compounds are confirmed by detailed scrutiny of the $^1\text{H-NMR}$ spectrum for the isolated regioisomeric mixture (~75/25: **C/B**). One can expect one singlet for **B**, two singlets for **C** and three singlets for **D** as depicted in Fig 4.

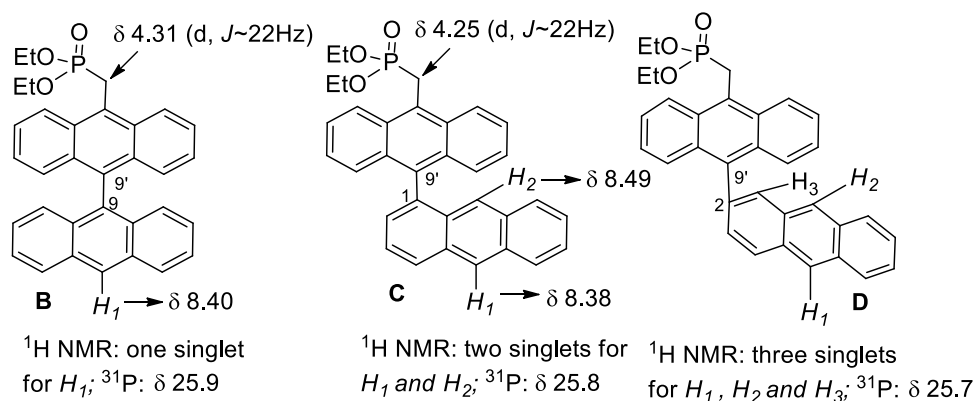


Fig 4 The number of singlet (s) possible for compounds **B-D** and assignment of the protons; **D** could not be isolated, ^{31}P NMR peak is assigned based on the reaction mixture ^{31}P -NMR. The formation of **D** is also not much supportive based on the mechanistic paths.

The isolated compound shows essentially two singlets at $\delta 8.49$ and 8.38 with equal peak area (Fig S15), indicating the presence of compound **C**. We could identify other singlets at $\delta 8.40$ (~25%, Fig S15) that might be originated from compound **B**. The ratio of regioisomeric mixture **C/B**: 75/25 is confirmed from both ^1H and ^{31}P NMR spectra (Fig S15 and S17). Mainly two signals at $\delta 25.8$ (~75%) and 25.9 (~25%) are found in the ^{31}P -NMR spectra for the isolated regioisomeric mixture, possibly for **C** and **B**, respectively. Based on our ^{31}P NMR of the reaction mixture, we can conclude that the regioisomer **D** perhaps resonates at $\delta 25.7$. However, we could not find the compound **D** as a part of our isolated regioisomeric mixture. In fact, the mechanistic pathway is more supportive of the formation of **B** and **C** in comparison to **D** (*vide infra*). Thus, we confirmed our isolated compound as a mixture of **C** (75%) and **B** (25%).

The mechanistic insights

Acid helps to generate the carbocation at the $\alpha\text{-C}$ *via* the activation of -OH functionality. The resulting carbocation **1aR** (Fig 5) is presumably unstable due to the electron-withdrawing effect of the phosphoryl group. However, being the immediate

carbocation (ion-pair concept), the attack to this carbocation is very much possible by anthracene ring before it gets stabilized through resonance. Interestingly, anthracene can attack from different carbon centers to form the intermediates **1aR1-1aR3** (Fig 5), in which the carbocation **1aR1** looks to be very much symmetrical and stable but experiences tremendous electronic repulsions and Van der Waals interactions between two anthracyl rings and that could be the reason for the nonexistence of the corresponding product. The formation of carbocation **1aR2** is not much favored due to the lack of stability through the mesomeric effect that disrupts the aromatic rings whereas the formation of the intermediate **1aR3** is more reasonable in terms of the stability through resonance even without disturbing the aromatic rings as well as avoiding the electronic repulsions between anthracyl π e's cloud and van der Waals interactions between peripheral H's. Thus, the compound **A** is originated from the most viable intermediate **1aR3**. We could not find the products that are expected to be formed from **1aR1** or **1aR2** intermediates and thus, the formation of such intermediates is expected to be uncertain.

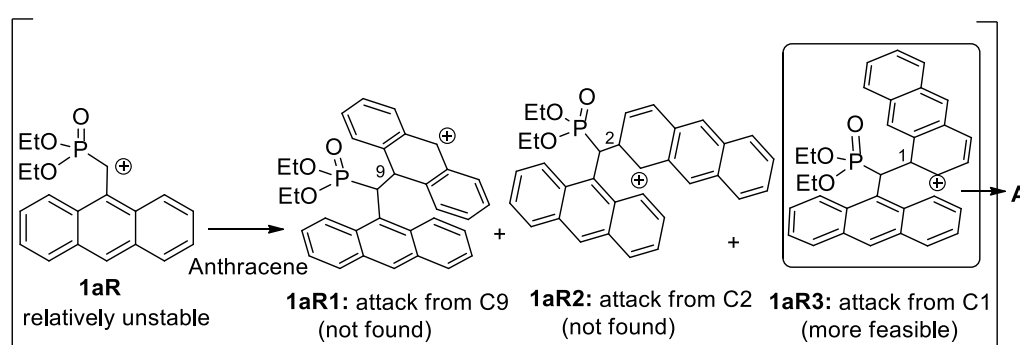


Fig 5. The possible intermediates through the attack at α -C; The intermediate **1aR3** produces **A**.

Next, we focus on the mechanism that likely leads to the formation of PCH_2 compounds **B-D** and the corresponding intermediates (**BI**, **CI**, and **DI**) are portrayed in Fig 6.

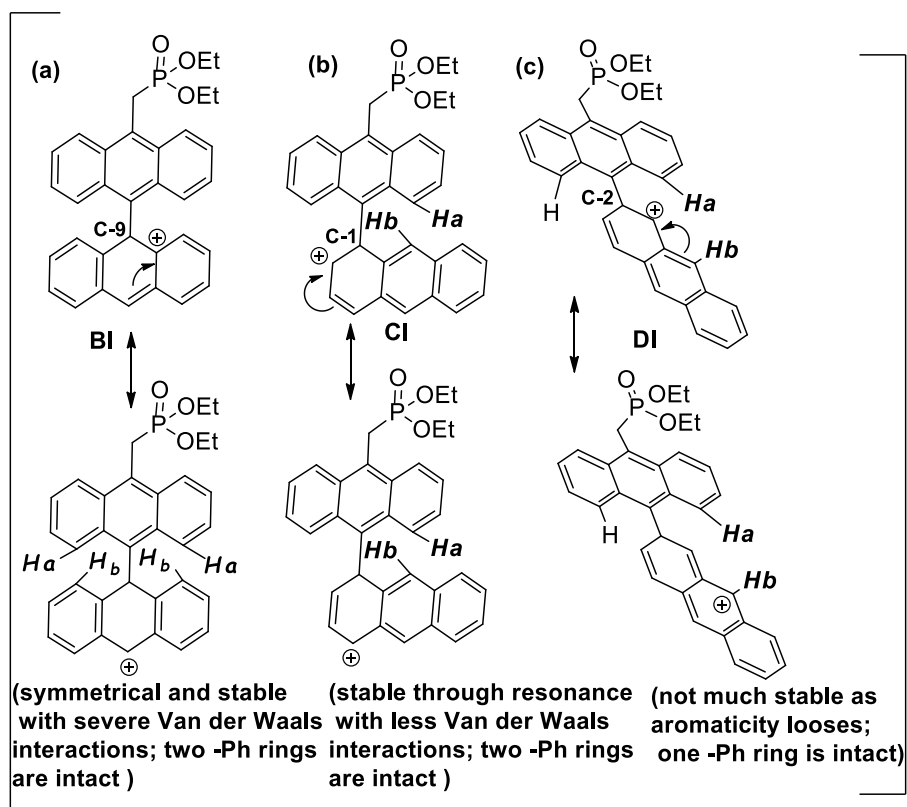


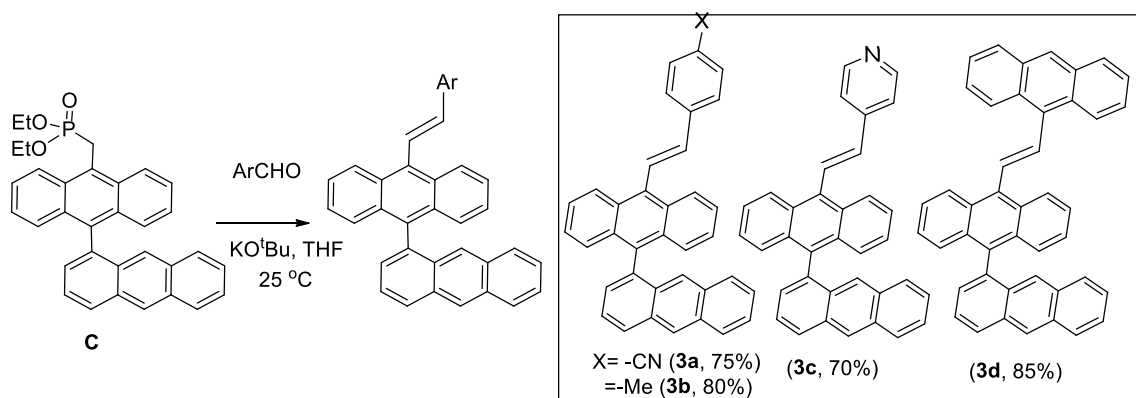
Fig 6. The possible intermediates and their stabilities through the attack at C-10.

The attack of most nucleophilic anthracenyl center C9 produced the carbocation **BI** that becomes most stable and symmetrical intermediate through resonance (with two intact aromatic rings) but severe van der Waals interactions from peripheral H's appear to be detrimental to produce **B** (Fig 6a). The next possible option to attack the carbocation through other nucleophilic carbon C1 and that form another stable intermediate **CI** (Fig 6b; resonance stability without disturbing the aromatic rings) where van der Waals interactions between H_a and H_b are also significantly minimized in comparison to **BI**. Thus, the formation of product **C** becomes more feasible. The other possible intermediate **DI** is formed through C2 attack (Fig 6c) and can be accounted for the formation of **D**. However, the stability of this intermediate is not much favored because the aromatic ring gets disturbed to attain the stability. Thus, considering the nucleophilic affinity of different carbon centers of anthracene as an arene, van der Waals interaction of the peripheral H's

and the resonance stability of the intermediates, the stability order (increasing) for these intermediates (Fig 6) can be demonstrated as **DI**<**BI**<**CI**. Thus, this explanation can further support the formation of compound **C** as major (~75%) and **B** as minor (~25%).

Applications in generating extensive π -conjugates:

Initially, we attempted the phosphonate **A** for HWE reactions with 4-bromobenzaldehyde by following our previous report^{7g} but no reactions were found even with the use of *n*-BuLi (Table S1). This might be due to the inaccessibility of *CH* proton, situated in the lap of two bulky anthracyl units and phosphoryl group. Even, the attempt to form ketone through oxy-Wittig reactions (reaction of carbanion with oxygen) was a failure.¹² As a much appropriate substrate, the regioisomeric mixture of P-CH₂ compounds [**B** (~25%)+**C** (~75%)] are applied for the HWE reactions and the olefin compounds **3a-d** with extended π -conjugation are isolated as regioisomeric mixture (Scheme 2). By varying the aldehydes in terms of electronic effects, the compounds were isolated in excellent yields. The pyridyl unit was introduced to obtain **3c** due to its ability to detect acid and metal ions.^{7b,8c,13} The tri-anthracyl π -conjugate was synthesized by using 9-anthraldehyde. As we started with a regioisomeric mixture of phosphonates, the π -conjugates are mostly isolated as regioisomeric mixture. However, to confirm the source **C** as phosphonate) (discussed in Fig 4), two expected singlets for anthracene rings are identified for olefins **3a** (δ 8.52 and 8.41), **3b** (δ 8.52, 8.38), **3c** (δ 8.52, 8.41) and **3d** (δ 8.54 and 8.44; actually there are two singlets at δ 8.44 as expected). The (*E*)-configuration was identified from the peaks of olefinic protons with coupling constant ~16 Hz. With these spectral analyses, we assign the structures for all these π -conjugates.



Scheme 2: Synthesis of π -conjugates **3a-d** as a regioisomeric mixture; being **C** is a major isolated product, another isomer **B** is not shown. The regioisomeric ratio: **3a**: could not be determined (peaks are merged), **3b-c**: ~75:25 and **3d**: ~95:5 (regioisomeric ratio) could be identified.

Aggregation-Induced Emission (AIE) studies

Even though the compounds are isolated as a regioisomeric mixture, our current interest in AIEgens⁷⁻⁸ insisted us to examine the AIE-properties for these extended π -conjugates (**3a-d**). To choose the water-miscible solvents for performing AIE-studies, the emission behavior of compound **3a** are examined in 1,4-dioxane, tetrahydrofuran (THF) and acetonitrile and the related parameters are tabulated in Table 2. The peak at $\lambda_{em}=510$ nm is less intense in acetonitrile (Fig S1). Therefore, acetonitrile is chosen as a good solvent to examine the enhancement in fluorescence intensity upon aggregation. Interestingly, the emission spectra are somewhat clean with majorly one sharp emission. The compound **3b** is the most fluorescing molecule while **3d** is the least (see Fig S2 and Table 2). It indicates a less quantum yield if the number of anthracyl unit within a molecule increases (additional number of flat and rigid rotors) and the compound **3b** possibly relaxes from pure LE state (locally excited) majorly through a radiative pathway. The emission maxima of **3a** at a higher wavelength (510 nm) can be accounted for the presence of the strong electron-withdrawing effect of $-\text{CN}$ functionality, imposing electronic push-pull effect. Even the

relatively longer wavelength emission was observed for **3c** due to the subtle electron-withdrawing effect of pyridyl moiety (Figure S3). Upon gradual increment of water fraction (water as bad solvent) to the acetonitrile solution of **3a**, the slight polarity effect on both absorption (5 nm redshift) and emission (8 nm redshift) was observed with the fluorescence quenching effect. Such fluorescence (Fl.) quenching may be attributed to the aggregation-caused quenching (ACQ) effect (see Fig S4) which is commonly observed for typical fluorescent molecules.¹⁴ Similar results were observed with compounds **3b-c**. The corresponding absorption and emission spectra of **3b-c** are presented in the ESI (Fig S5-S6, Table 2). Thus, the compounds **3a-c** showed ACQ behavior similar to the usual fluorophores.

Table 2: Parameters for the photophysical studies of compounds **3a-d** (regioisomeric mixture). All quantum yields (QY) are calculated with a reference of quinine sulfate in 0.1M H₂SO₄. Error in quantum yield calculations: $\pm 5\%$.

Compound		3a	3b	3c	3d
Molecular form (in solution)	λ_{abs}	399	397	398	403
	λ_{em}	510	489	501	487
	QY %	7.2	12.5	7.3	0.8
Aggregate form ($f_w=90$ v/v%)	λ_{abs}	405	402	403	410
	λ_{em}	518	512	513	539
	QY %	5.6	3.9	1.7	2.6
I/I_0 ($f_w=90$ v/v%)		0.70	0.29	0.12	2.15
α_{AIE} (AIE measurement parameter)= 2.6/0.8		--	--	--	3.25

On the contrary, we observed an increase in fluorescence intensity with a redshift of 52 nm for the compound **3d** (487 nm to 539 nm; Figure 7). Such a shift with enhanced Fl. intensity illustrate the molecular aggregation that favors the electronic

conjugations along with restricted intramolecular motions, which established as an origin of the AIE-effect.^{7e-f}

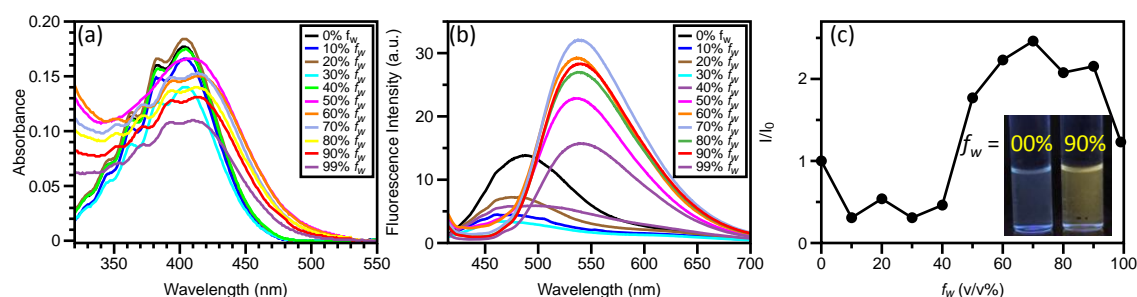


Fig 7: (a) absorption spectra (b) emission spectra (c) f_w (v/v%) spectra of compound **3d** 10 μ M in acetonitrile. λ_{ex} = 405 nm.

The multiple anthracyl units might have restricted intramolecular rotation (RIR) of the molecule in the aggregate state to result in the enhanced fluorescence. The particle size of **3d** was determined through DLS study and appeared to be 156 nm, which supports the formation of nano-aggregates.¹⁵ To further confirm the RIR effect, the emission spectra are recorded individually in MeOH and more viscous MeOH/glycerol (1/1) medium where the FI. intensity was boosted (Fig S7) almost two times. The rotation is more restricted in viscous medium and therefore the FI. intensity is enhanced. Further, the presence of three anthracyl rings will have a tendency to form excimer and therefore concentration-dependent FI. studies are also conducted (Fig S8). The structured bands at \sim 455 nm appeared in the emission spectrum for the 10^{-9} M solution. On increase the concentration, there was a signature at 513 nm and that kept increasing till 10^{-7} M. However, the emission at 10^{-5} M showed the band at λ_{max} = 460 nm which can be attributed to monomer. However, this study was not much conclusive in this case. Thus, we envisage that the aggregate formation has increased the planarity of the system to enhance the electronic conjugation that results in red-shift and the RIR effect is responsible for the enhancement in the FI. intensity.

Conclusion

In conclusion, we have established simple but effective FC-type arylation reaction to afford a variety of anthracene substituted anthracylphosphonates. The product by anthracene attack at α -C of anthracylphosphonate through C1 is recognized by X-ray structure and explained with a light of stability of the corresponding intermediate. This compound shows one of the bond angles is 118° , which is not usual for sp^3 hybridized carbon. The formation of other possible diverse products with PCH_2 motif is also identified. The effort has been made to isolate, characterize and maximize the yield of majorly formed phosphonates. The phosphonate with $-PCH_2$ motif has been successfully utilized in HWE reactions to generate bis or tris-anthracyl linked extensive π -conjugates in good yields. These molecules are found somewhat fluorescent with ACQ behavior except tris-anthracyl π -conjugate that showed the AIE behavior. The photophysical property in terms of exhibiting AIE-behaviour was not highly impressive. Thus, we have established that the enhanced number of anthracene rings for such system could be detrimental for exhibiting the AIE-properties.

Experimental

General Consideration: Reagents

All experiments were carried out in hot air oven-dried glassware under nitrogen, argon or oxygen atmosphere. Diethyl ((10-(*aryl*)anthracen-9-yl)methyl)phosphonates were prepared in our lab using the reported procedure.^{5a} Potassium *tert*-butoxide (KO^tBu) was purchased from Aldrich and used as received. THF was redistilled from sodium metal and benzophenone mixture. All other reagents were purchased from common suppliers and used without further purification. Column chromatography was performed using Silica gel 100-200 mesh. Reactions were monitored by thin-layer

chromatography on pre-coated with silica gel 60 F₂₅₄ plates (Merck & Co.) and were visualized by UV- light (~365 nm).

Analytical Methods:

¹H, ¹³C-NMR spectra were recorded in CDCl₃ solution using Bruker Avance DRX (400 and 500 MHz). The signals were referenced to TMS and solvent used is deuterated chloroform (7.26 ppm in ¹H, 77.16 ppm ¹³C). Chemical shifts are reported in ppm, multiplicities are indicated by s (singlet), d (doublet), t (triplet), dd (doublet of a doublet). The fluorescence spectra were recorded on a Shimadzu spectrofluorimeter. The electronic absorption spectra were recorded with UV-Vis Scanning spectrophotometer. ESI-LCMS was recorded in Shimadzu LCMS-2020. The X-ray quality crystals of the compounds were grown by slow diffusion of *n*-hexane over CH₂Cl₂ or *n*-hexane over ethyl acetate solution. The single-crystal X-ray data were collected on a Rigaku XtaLAB Pro 200 diffractometer using graphite monochromated Mo or Cu radiation. Data were collected and processed using CrysAlisPro (Rigaku Oxford Diffraction). The structures were solved by direct methods and refined by a full-matrix least-squares method using standard procedures. Absorption corrections were done using Lorentz and polarization effects, where applicable. In general, all non-hydrogen atoms were refined anisotropically; hydrogen atoms were fixed by geometry or located by a difference Fourier map and refined isotropically. All bond angles, bond or other distances and dihedral angles are determined using mercury 3.3 software. DLS particle size analysis was carried out using a Zetasizer Nano S from Malvern Instruments at 25 °C.

Diethyl (anthracen-1-yl(anthracen-9-yl)methyl)phosphonate: (A)

In a 50 mL round bottomed flask, diethyl (anthracen-9-yl(hydroxy)methyl)phosphonate (1.00 g, 2.904 mmol) and anthracene (0.517 g, 2.904 mmol) were taken and dissolved in dichloromethane. Then, methanesulfonic acid

(0.614 g, 6.389 mmol) was added and the reaction was allowed to stir for 2 h under nitrogen balloon. The completion of reaction was monitored by TLC. The reaction mixture was quenched with water and extracted with dichloromethane (30 mL x 3). The organic layer was filtered and dried over anhydrous sodium sulphate and evaporated under reduced pressure. The compound **A** was purified by column chromatography using 30% ethyl acetate in petroleum ether. $R_f = 0.4$ (30% ethyl acetate in hexane), colorless crystals, mp (176-180 °C); yield 0.395 g (27%). IR (KBr, cm^{-1}) 3471, 3052, 2982, 1620, 1557, 1447, 1322, 1229, 1049, 1020, 966, 869, 787, 729. ^1H NMR (500 MHz, CDCl_3) δ 9.09-8.85 (m, 2H), 8.82 (d, $J = 7.1$ Hz, 1H), 8.41-8.33 (m, 1H), 8.24 (s, 1H), 8.09 (d, $J = 14.1$ Hz, 2H), 7.94-7.71 (m, 4H), 7.70-7.54 (m, 2H), 7.25-7.19 (m, 3H), 7.17-7.08 (m, 1H), 7.01 (d, $J = 8.5$ Hz, 1H), 6.82 (d, $J = 30.4$ Hz, 1H), 4.27 (h, $J = 7.2$ Hz, 2H), 3.77 – 3.54 (m, 1H), 3.23 – 2.95 (m, 1H), 1.33 (t, $J = 7.1$ Hz, 3H), 0.66 (t, $J = 7.0$ Hz, 3H). ^{13}C NMR (126 MHz, CDCl_3) δ 134.34, 132.01 (d, $J = 5.7$ Hz), 131.99, 131.54, 131.22, 130.7 (d, $J = 15.0$ Hz), 130.12, 128.84 (d, $J = 4.7$ Hz), 128.6 (d, $J = 8.0$ Hz), 128.53, 128.34 (d, $J = 5.0$ Hz), 127.37, 127.08, 126.97, 125.38, 125.08, 124.98, 124.67, 124.46, 124.19, 123.96, 123.46, 63.04 (d, $J = 6.8$ Hz), 62.26 (d, $J = 7.3$ Hz), 43.33 (d, $J = 142.1$ Hz), 16.2 (dd, $J = 56.9, 5.9$ Hz). ^{31}P NMR (162 MHz, CDCl_3) δ 25.6; LC/MS: m/z 505 $[\text{M}+\text{H}]^+$. X-ray crystal data is done for this sample. (CCDC NO 1898082).

Diethyl ([2,9'-bianthracen]-10'-ylmethyl)phosphonate: (C)

In a 50 mL round bottomed flask, diethyl (anthracen-9-yl(hydroxy)methyl)phosphonate (1.00 g, 2.904 mmol) and anthracene (0.517 g, 2.904 mmol) were taken and dissolved in dichloromethane. Then, triflic acid (0.872 g, 5.808 mmol) was added and the reaction was allowed to stir for 2 h under nitrogen balloon. The completion of reaction was monitored by TLC. The reaction mixture was quenched with water and extracted with dichloromethane (30 mL x 3). The organic

layer was filtered and dried over anhydrous sodium sulphate and evaporated under reduced pressure. The compound **D** was purified by column chromatography using 40% ethyl acetate in petroleum ether. The compound was isolated as regioisomeric mixture (75:25); $R_f = 0.3$ (40% ethyl acetate in hexane), pale yellow fluffy solid, mp (82-86 °C); yield 0.878 g (60%). IR (KBr, cm^{-1}) 3748, 2979, 1671, 1624, 1558, 1322, 1444, 1376, 1248, 1161, 1053, 1022, 962, 884, 764. ^1H NMR (400 MHz, CDCl_3) δ 8.49 (s, 1H), 8.38 (s, 1H), 8.36 (d, $J = 8.8$ Hz, 2H), 8.11 (t, $J = 7.9$ Hz, 1H), 7.99 – 7.91 (m, 2H), 7.67 (d, $J = 8.8$ Hz, 1H), 7.52 – 7.36 (m, 6H), 7.35 – 7.21 (m, 2H), 7.16 – 7.00 (m, 1H), 4.25 (d, $J = 22.5$ Hz, 2H), 3.98 – 3.81 (m, 4H), 1.08 (t, $J = 7.1$ Hz, 6H). The doublet at δ 4.31 ($J = 22.5$ Hz) due to other isomer was observed. ^{13}C NMR (101 MHz, CDCl_3) δ 137.4 (d, $J = 6.1$ Hz), 136.0, 132.2, 132.0, 131.5, 130.9, 130.2, 129.3, 128.4 (d, $J = 2.9$ Hz), 128.3, 128.2, 128.1, 127.7, 126.6, 126.4 (d, $J = 14.5$ Hz), 125.73, 125.6, 125.5, 125.3, 125.2, 125.1, 123.9 (d, $J = 11.3$ Hz), 62.29 (d, $J = 6.7$ Hz), 27.3 (d, $J = 140.7$ Hz), 16.37 (d, $J = 6.0$ Hz). The doublet at δ 27.4 ($J = 140.7$ Hz) due to the other isomer was observed. ^{31}P NMR (162 MHz, CDCl_3) δ 25.8; The other isomer (assumed to be **C**) appeared at δ 25.7 in ^{31}P NMR. LC/MS: m/z 505 $[\text{M}+\text{H}]^+$.

(E)-4-(2-([2,9'-bianthracen]-10'-yl)vinyl)benzotrile: 3a

In a 25 mL round bottomed flask, compound **C** (0.1 g, 0.198 mmol) was taken and dissolved in dry THF. Then potassium tert-butoxide (0.066 g, 0.594 mmol) was added and the reaction was allowed to stir for 2 min under nitrogen balloon. Then 4-formylbenzotrile (4-cyanobenzaldehyde) was added and the reaction was allowed to stir for 2h. The completion of reaction was monitored by TLC. The reaction mixture was quenched with water and extracted with ethylacetate (20 mL x 3). The organic layer was filtered and dried over anhydrous sodium sulphate and evaporated under reduced pressure. The compound **3a** was purified by column chromatography using

2% ethyl acetate in petroleum ether. The compound was isolated as pale greenish yellow solid, mp (272-276 °C); yield 0.071 g (75%). IR (KBr, cm^{-1}) 3445, 2922, 2851, 2223, 1602, 1458, 1261, 1029, 806, 754. ^1H NMR (400 MHz, CDCl_3) δ 8.52 (s, 1H), 8.41 (s, 1H), 8.35- 8.29 (m, 1H), 8.19 – 8.06 (m, 2H), 8.03 (d, $J = 5.5$ Hz, 1H), 7.96 (t, $J = 7.8$ Hz, 1H), 7.70-7.76 (m, 5H), 7.64–7.57 (m, 1H), 7.48 – 7.38 (m, 5H), 7.36 – 7.25 (m, 2H), 7.23 – 7.19 (m, 1H), 7.17 – 7.13 (m, 1H), 6.97 (d, $J = 16.5$ Hz, 1H). ^{13}C NMR (101 MHz, CDCl_3) δ 141.6, 135.9, 135.8, 132.7, 132.7, 131.9, 131.0, 130.9, 130.3, 130.2, 129.4, 129.3, 129.2, 128.7, 128.5, 128.3, 128.2, 127.9, 127.7, 127.6, 127.1, 126.5, 126.3, 125.7, 125.6, 125.5, 125.4, 119.01, 111.35. LC/MS: m/z 481 $[\text{M}]^+$. HR-MS (ESI): expected $\text{C}_{37}\text{H}_{23}\text{N}$ 481.1830, found 481.1832 $[\text{M}]^+$.

(E)-10'-(4-methylstyryl)-2,9'-bianthracene (**3b**): Compound **3b** was synthesized in a fashion similar to compound **3a**. Compound **C** (0.1 g, 0.198 mmol) potassium tert-butoxide (0.066 g, 0.594 mmol) and 4-methylbenzaldehyde were used. The compound **3b** was purified by column chromatography using 2% ethyl acetate in petroleum ether. The compound was isolated as pale yellow solid, mp (246-250 °C); yield 0.075 g (80%). IR (KBr, cm^{-1}) 3640, 2956, 2922, 2848, 1715, 1556, 1507, 1456, 1261, 1028, 805, 752. ^1H NMR (400 MHz, CDCl_3) δ 8.52 (s, 1H), 8.41-8.40 (m, 1H), 8.38 (s, 1H), 8.14 (d, $J = 8.8$ Hz, 1H), 8.03 – 7.95 (m, 3H), 7.88 (d, $J = 16.5$ Hz, 1H), 7.69 (d, $J = 8.7$ Hz, 1H), 7.59 – 7.53 (m, 2H), 7.49-7.43 (m, 4H), 7.41 – 7.37 (m, 3H), 7.29-7.27 (m, 2H), 7.25 – 7.21 (m, 2H), 6.91 (d, $J = 16.5$ Hz, 1H), 2.38 (s, 3H). ^{13}C NMR (126 MHz, CDCl_3) δ 137.0, 136.4, 135.5, 135.0, 133.6, 132.3, 131.1, 130.9, 130.5, 129.9, 129.2, 129.1, 128.5, 128.4, 128.4, 127.2, 127.1, 126.2, 125.5, 125.4, 125.3, 125.2, 124.6, 124.5, 124.4, 124.2, 124.1, 123.0, 28.6. LC/MS: m/z 471 $[\text{M}+\text{H}]^+$. HR-MS (ESI): expected $\text{C}_{37}\text{H}_{26}$ 470.2035, found 470.1970 $[\text{M}]^+$.

(E)-4-(2-([2,9'-bianthracen]-10'-yl)vinyl)pyridine (**3c**): Compound **3c** was synthesized in a fashion similar to compound **3a**. Compound **C** (0.1 g, 0.198 mmol) potassium

tert-butoxide (0.066 g, 0.594 mmol) and 4-pyridine carboxaldehyde were used. The compound **3c** was purified by column chromatography using 12% ethyl acetate in petroleum ether. The compound was isolated as pale yellow solid, mp (152-156 °C); yield 0.063 g (70%). IR (KBr, cm⁻¹) 3748, 3647, 3027, 2924, 2848, 1715, 1593, 1541, 1456, 1210, 1021, 967, 881, 739. ¹H NMR (400 MHz, CDCl₃) δ 8.64 – 8.63 (m, 2H), 8.52 (s, 1H), 8.41 (s, 1H), 8.46 – 8.38 (m, 2H), 8.31 – 8.29 (m, 2H), 8.16 – 8.13 (m, 2H), 8.04 – 8.01 (m, 1H), 7.72 (d, *J* = 8.7 Hz, 2H), 7.52 – 7.50 (m, 1H), 7.48 – 7.43 (m, 4H), 7.42 – 7.40 (m, 2H), 7.30-7.26 (m, 2H), 6.91 (d, *J* = 16.6 Hz, 1H). ¹³C NMR (101 MHz, CDCl₃) δ 150.3, 144.5, 137.6, 135.7, 135.1, 132.2, 132.0, 131.6, 131.5, 130.9, 130.2, 130.1, 129.3, 129.2, 128.3, 128.2, 127.9, 127.8, 127.7, 127.5, 126.4, 126.3, 125.8, 125.7, 125.6, 125.4, 121.1. LC/MS: *m/z* 458 [M+H]⁺. HR-MS (ESI): expected C₃₅H₂₄N 458.1909, found 458.1907 [MH]⁺.

(E)-10'-(2-(anthracen-9-yl)vinyl)-2,9'-bianthracene: **3d**

Compound **3d** was synthesized in a fashion similar to compound **3a**. Compound **C** (0.1 g, 0.198 mmol) potassium tert-butoxide (0.066 g, 0.594 mmol) and 9-anthraldehyde were used. The compound **3d** was purified by column chromatography using 2% ethyl acetate in petroleum ether. The compound was isolated as pale orange red solid, mp (210-214 °C); yield 0.094 g (85%). IR (KBr, cm⁻¹) 3048, 2922, 2851, 1518, 1440, 1380, 1215, 987, 885, 732. ¹H NMR (400 MHz, CDCl₃) δ 8.66 (d, *J* = 8.8 Hz, 2H), 8.64 – 8.59 (m, 2H), 8.54 (s, 1H), 8.44 (s, 2H), 8.17 (d, *J* = 9.0 Hz, 1H), 8.09 – 8.06 (m, 1H), 8.05 – 8.01 (m, 3H), 8.00 – 7.96 (m, 1H), 7.88-7.87 (m, 2H), 7.77 (d, *J* = 8.7 Hz, 2H), 7.54 – 7.49 (m, 2H), 7.48 – 7.46 (m, 5H), 7.43- 7.42 (m, 2H), 7.34-7.30 (m, 2H). ¹³C NMR (101 MHz, CDCl₃) δ 136.0, 134.9, 132.9, 132.8, 132.0, 131.7, 131.1, 131.0, 130.6, 130.5, 129.9, 129.3, 129.2, 128.7, 128.4, 128.3, 127.9, 127.8, 127.2, 127.2, 126.5, 126.4, 125.8, 125.4, 125.3,

125.1, 124.9, 124.8, 124.6, 124.5, 124.3, 124.2. LC/MS: m/z 557 [M+H]⁺. HR-MS (ESI): expected C₄₄H₂₈ 556.2191, found 556.2106 [M]⁺.

Supporting Information

File Name: Supporting Information_MC

File Format: Word

Acknowledgements

We specially thank the reviewers for their constructive comments. We thank CSIR [02(289)/17] for financial support. The DST-FIST facility is also partially accredited. The BITS-Pilani Hyderabad campus crystallographic and NMR facility is highly acknowledged.

References

1. (a) Dong, J.; Liu, W.; Ying, S.; Wu, Y.; Xue, S.; Yang, W. *J Lumines*, **2016**, 176, 168. (b) Kraicheva, I.; Vodenicharova, E.; Shivachev, B.; Nikolova, R.; Kril, A.; Topshka Ancheva, M.; Iliev, I.; Georgieva, A.; Gerasimova, T.; Tosheva, T.; Tashev, E.; Tsacheva, I.; Troev, K. *Phosphorus, Sulfur and Silicon and the relat elem.*, **2013**, 188, 1535. (c) Zhang, X.; Chi, Z.; Zhang, J.; Li, H.; Xu, B.; Li, X.; Liu, S.; Zhang, Y.; Xu, J. *J. Phys. Chem. B* **2011**, 115, 7606.
2. (a) Pramanik, M.; Chatterjee, N.; Das, S.; Saha, K. D.; Bhaumik, A. *Chem. Commun.*, **2013**, 49, 9461. (b) Cao, D. K.; Gu, Y. W.; Feng, J. Q.; Cai, Z. S.; Ward, M. D. *Dalton Trans.*, **2013**, 42, 11436.

3. (a) Yoshizawa, M.; Losterman, J. K. *Chem. Soc. Rev.*, **2014**, *43*, 1885. (b) Huang, J.; Su, J.-H.; Tian, H. *J. Mater. Chem.*, **2012**, *22*, 10977. (c) Lee, J. H.; Ham, H. W.; An, H. C.; Kim, D. J.; Han, J. W.; Gim, G. T. Patent number WO 2014003405, **2014** Jan 3
4. (a) Ogata, F.; Takagi, M.; Nojima, M.; Kusabayashi, S. *J. Am Chem Soc.* **1982**, *103*, 1145. (b) Panda, G.; Mishra, J. K.; Shagufta; Dinadayalane, T. C.; Narahari Sastry, G.; Negi, D. S. *Ind. J. of Chem.* **2006**, *45B*, 276.
5. (a) Baig, M. Z. K.; Pallikonda, G.; Trivedi, P.; Tulichala, R. N. P.; Ghosh, B.; Chakravarty, M.; *ChemistrySelect*, **2016**, *1*, 4332. (b) Luo, J.; Xie, Z.; Lam, J. W. Y.; Cheng, L.; Tang, B. Z.; Chen, H.; Qiu, C.; Kwok, H. S.; Zhan, X.; Liu, Y. *Chem. Comm.*, **2001**, 1740.
6. (a) Kumaraswamy, K. C.; Srinivas, V.; Pavan Kumar, K. V. P.; Praveen Kumar, K. *Synthesis* **2007**, *6*, 893. (b) Cao, D.; Lu, Y. H.; Zheng, T.; Zhang, Y. H.; Li, Y. Z.; Zheng, L. M. *RSC Adv.*, **2013**, *3*, 4001. (c) Tang, B. Z.; Zhan, X.; Yu, G.; Sze Lee, P. P.; Liu, Y.; Zhu, D. *J. Mater. Chem.*, **2001**, *11*, 2974.
7. (a) Baig, M. Z. K.; Majhi, D.; Tulichala, R. N. P.; Sarkar, M.; Chakravarty, M. *J. Mater. Chem. C.* **2017**, *5*, 2038. (b) Baig, M. Z. K.; Pawar, S.; Tulichala, R. N. P.; Nag A.; Chakravarty, M. *Sensor Actuat B Chem.* **2017**, *243*, 226. (c) Chiang, C. J.; Kimyonok, A.; Etherington, M. K.; Griffiths, G. C.; Jankus, V.; Turksoy, F.; Monkman, A. P. *Adv. Funct. Mater.*, **2012**, 739. (d) Aydemir, M.; Haykir, G.; Battal, A.; Jankus, V.; Sugunan, S. K.; Dias, F.B.; Al-Attar, H.; Türksoy, F.; Tavasli, M.; Monkman, A. P. *Org. Electronics*, **2016**, *30*, 149. (e) Hong, Y.; Lam, J. W. Y.; Tang, B. Z. *Chem. Soc. Rev.*, **2011**, *40*, 5361. (f) Hong, Y.; Lam, J. W. Y.; Tang, B. Z. *Chem. Commun.* **2009**, *29*, 4332. (g) Baig, M. Z. K.; Sahu, P. K.; Sarkar, M.; Chakravarty, M. *J. Org. Chem.* **2017**, *82*, 13359.
8. (a) Baig, M. Z. K.; Prusti, B.; Roy, D.; Sahu, P. K.; Sarkar, M.; Sharma, A.; Chakravarty, M. *ACS Omega*, **2018**, *3*, 9114. (b) Baig, M. Z. K.; Prusti, B.; Sandeep,

- K.; Chakravaty, M. *J Lumines.* **2014**, *209*, 188. (c) Baig, M. Z. K.; Prusti, B.; Chakravarty, M. *J. Mater. Chem. C*, **2019**, *7*, 3735.
9. (a) Kumar, R.; Van der Eycken, E. V. *Chem Soc. Rev.* **2013**, *42*, 1121. (b) Tsuchimoto, T.; Tobita, K.; Hiyama, T.; Fukuzawa, S. *J. Org. Chem.* **1997**, *62*, 6997. (c) Sanz, R.; Martínez, A.; Miguel, D. J. M.; Gutiérrez, Á.; Rodríguez, F. *Adv. Synth. Catal.* **2006**, *348*, 1841. (d) Mo, X.; Yakiwchuk, J.; Dansereau, J.; McCubbin, J. A.; Hall, D. G. *J. Am. Chem. Soc.* **2015**, *137*, 9694.
10. (a) Xu, B. J.; Chi, Z. G.; Yang, Z. Y.; Chen, J. B.; Deng, S. Z.; Li, H. Y.; Li, X. F.; Zhang, Y.; Xu, N. S.; Xu, J. R. *J. Mater. Chem.*, **2010**, *20*, 4135. (b) Mei, J.; Leung, N. L. C.; Kwok, R. T. K.; Lam, J. W. Y.; Tang, B. Z. *Chem. Rev.* **2015**, *115*, 11718. (c) Qin, A.; Tang, B. Z. *Aggregation Induced Emission: Applications*, 1st Edition, John Wiley & Sons, **2014**.
11. Pallikonda, G.; Chakravarty, M. *Eur. J. Org. Chem.*, **2013**, *5*, 944.
12. Zubair, M. K. B.; Pallikonda, G.; Tulichala, R. N. P.; Chakravarty, M.; *Tetrahedron*, **2016**, *72*, 2094.
- 13 (a) Dong, Y.; Xu, B.; Zhang, J.; Tan, X.; Wang, L.; Chen, J.; Lv, H.; Wen, S.; Li, B.; Ye, L.; Zou, B.; Tian, W. *Angew. Chem. Int. Ed.*, **2012**, *51*, 10782. (b) Zhang, J.; Chen, J.; Xu, B.; Wang, L.; Ma, S.; Dong, Y.; Li, B.; Ye, L.; Tian, W. *Chem. Commun.*, **2013**, *49*, 3878. (c) Dong, Y.; Zhang, J.; Tan, X.; Wang, L.; Chen, J.; Li, B.; Ye, L.; Xu, B.; Zoub, B.; Tian, W. *J. Mater. Chem. C*, **2013**, *1*, 7554.
14. (a) Thomas III, S. W.; Joly, G. D.; Swager, T. M. *Chem. Rev.* **2007**, *107*, 1339. (b) Belletete, M.; Bouchard, J.; Leclerc, M.; Durocher, G. *Macromolecules*, **2005**, *38*, 880.
15. An, B. K.; Kwon, S. K.; Jung, S. D.; Park, S. Y. *J. Am. Chem. Soc.* **2002**, *124*, 14410.